Parallel Poly-adenine Duplex Formation at Low pH Facilitates DNA Conjugation onto Gold Nanoparticles

Zhicheng Huang, Biwu Liu, and Juewen Liu*

Department of Chemistry, Waterloo Institute for Nanotechnology, University of Waterloo,

Waterloo, Ontario, N2L 3G1, Canada

Email: liujw@uwaterloo.ca

Abstract

DNA-functionalized gold nanoparticles (AuNPs) have been extensively used in sensing, drug delivery, and materials science. A key step is to attach DNA to AuNPs forming a stable and functional conjugate. While the traditional salt-aging method takes a full day or longer, a recent low-pH method allows DNA conjugation in a few minutes. The effect of low pH was attributed to protonation of adenine (A) and cytosine (C), resulting in an overall lower negative charge density on DNA. In this work, the effect of DNA conformation at low pH is studied. Using circular dichroism (CD) spectroscopy, parallel poly-A duplex (A-motif) is detected when a poly-A segment is linked to a random DNA, a design typically used for DNA conjugation. A DNA staining dye, thiazole orange, is identified for detecting such A-motifs. The A-motif structure is ideal for DNA conjugation since it exposes the thiol group for directly reacting with gold surface while minimizing non-specific DNA base adsorption. For non-thiolated DNA, the optimal procedure is to incubate DNA and AuNPs followed by lowering the pH. The i-motif formed by poly-C DNA at low pH is less favorable for the conjugation reaction due to its unique way of folding. The stability of poly-A and poly-G DNA in low pH is examined. An excellent stability of poly-A DNA is confirmed, while poly-G has lower stability. This study provides new fundamental insights into a practically useful technique of conjugating DNA to AuNPs.

Introduction

The interaction between DNA and gold nanoparticles (AuNPs) is an interesting biointerface topic with applications in analytical chemistry,[1-6] drug delivery,[7, 8] and materials science.[9-12] AuNPs have a strong inter-particle van der Waals force, and citrate-capped AuNPs are only stabilized by weak electrostatic repulsion, rendering them easily aggregated at a slightly elevated ionic strength. Thiolated DNA is the most commonly used reagent for functionalizing AuNPs due to the strong thiol-Au interaction.[13] The colloidal stability of AuNPs is significantly improved upon DNA conjugation.

Between the thiol group and the DNA sequence intended for hybridization, a polynucleotide spacer is often added. Historically, the Mirkin group used a poly-A spacer for many years, and this has been followed by many others. Further studies showed that a poly-A DNA binds to gold surfaces quite strongly,[14, 15] and the more weakly interacting poly-T spacers support the highest DNA loading density.[16] Regardless of the spacer sequence, in a typical conjugation reaction, thiolated DNA is mixed with AuNPs and the NaCl concentration is gradually raised to ~300 mM over a few hours to a day to achieve a stable conjugate.[17]

In 2012, we studied the adsorption of DNA by AuNPs and identified the critical role of pH,[18] allowing DNA conjugation reaction in a few minutes at pH 3.[19] The same method was also successfully applied to larger AuNPs,[20, 21] Au nanorods,[22] silver NPs,[23] and platinum NPs.[24] Quite interestingly, a high density of non-thiolated DNA with a poly-A fragment can also be adsorbed at low pH.[25]

We explained the pH effect mainly based on charge. Adenine (pK_a = 3.5) can be protonated at pH 3.0, which decreases the negative charge density on DNA and facilitates DNA adsorption.

However, this simple charge model cannot account for all the observations. 1) Based on the salt-aging model, DNA should first lie down on AuNPs since DNA bases can also bind to gold strongly.[13, 17] Gradually, the adsorbed DNA stands up due to displacement by the thiol group from the new incoming DNA. Introducing a positive charge to DNA bases should even promote DNA base adsorption. 2) More surprisingly, we achieved a high loading density of non-thiolated poly-A DNA similar to that for thiolated DNA (e.g. >60 poly-A DNA per 13 nm AuNP).[25, 26] Without a thiol group, DNA is expected to wrap around AuNPs,[27-31] which should limit its density. Therefore, other reasons must also be considered beyond simple protonation of DNA bases.

At low pH, DNA adopts different conformations beyond those based on the typical Watson-Crick base pairing, which may also affect the adsorption process. A well-known example is the i-motif formed by poly-C DNA. Poly-A DNA can form parallel duplexes in acidic pH.[32, 33] In this work, we aim to understand the effect of DNA conformation at low pH and its effect on the AuNPs conjugation reaction. In particular, we focus on the poly-A parallel duplex.

Materials and Methods

Chemicals. All the DNA samples were from Integrated DNA Technologies (IDT, Coralville, IA). Their sequences and modifications are listed in Table 1. SYBR Green I (SGI) was from Invitrogen (Carlsbad, CA). Thiazole orange (TO), $HAuCl_4$ and KCN were from Sigma-Aldrich. Ethanol, sodium hydroxide, and hydrochloric acid were from VWR (Mississauga, ON). Ethidium bromide (EB), sodium chloride, sodium citrate, and 4-(2-hydroxyethyl) piperazine-1-ethanesulfonate (HEPES) were from Mandel Scientific (Guelph, ON). AuNPs (13 nm diameter) were synthesized following literature reported procedure, and the as-prepared AuNPs were ~10 nM.[34]

Table 1. A list of the DNA sequences and modifications used in this work. FAM = carboxyfluorescein.

DNA ID	DNA Names	Sequences and modifications (from 5′ to 3′)
1	A_0-DNA	TTCACAGATGCGT
2	A_3-DNA	TTCACAGATGCGTAAA
3	A_9-DNA	TTCACAGATGCGTAAAAAAAAA
4	A_{15}-DNA	TTCACAGATGCGTAAAAAAAAAAAAAAA
5	C_0-DNA	TTTCACAGATGCGT
6	C_3-DNA	TTTCACAGATGCGTCCC
7	C_9-DNA	TTTCACAGATGCGTCCCCCCCCC
8	C_{15}-DNA	TTTCACAGATGCGTCCCCCCCCCCCCCCC
9	A_{15}	AAAAAAAAAAAAAAA
10	T_{15}	TTTTTTTTTTTTTTT
11	G_{15}	GGGGGGGGGGGGGGG
12	C_{15}	CCCCCCCCCCCCCCC
13	A_{10}-FAM	AAAAAAAAAA-FAM
14	A_{15}-FAM	AAAAAAAAAAAAAAA-FAM
15	FAM-DNA	FAM-ACGCATCTGTGA
16	5′SH-A_9-DNA	SH-AAAAAAAAACCCAGGTTCTCT
17	3′SH-A_9-DNA	TCACAGATGCGTAAAAAAAAA-SH

CD spectroscopy. CD spectroscopy was performed in a 1 cm UV−vis quartz cuvette using a Jasco J-715 Spectrophotometer. Two 5 mM citrate buffer (pH 3.0 and 7.0) samples were measured as blanks. Each DNA sample (10 μM, 200 μL) was dissolved in 5 mM citrate buffer and was measured 10 times with the continuous scanning mode (100 nm/min) from 200 to 300 nm.

DNA staining. DNA samples (1 μM) were respectively incubated in 50 mM citrate buffers (pH 3.0 and pH 7.0) for 5 min. Then DNA staining dyes (EB, SGI, and TO) were respectively added

(final dye concentration = 15 μM). The fluorescent signal was collected on a Varian Eclipse fluorometer under different excitation wavelengths (510 nm for TO, 520 nm for EB, and 485 nm for SGI).

DNA density and AuNP stability measurement. The process of preparing DNA-functionalized AuNPs was the same regardless of the DNA sequences or modification. First, a DNA solution (100 mM, 2 μL) was mixed with 100 μL as-synthesized 13 nm AuNPs. After 3 min incubation, the mixture was adjusted to pH 3.0 by adding citrate buffer (500 mM, pH 3.0, 2 μL). After 3 min, the mixture was adjusted back to neutral by adding HEPES buffer (500 mM, pH 7.0, 6 μL). Finally, the resulting DNA-functionalized AuNPs were washed with 5 mM HEPES buffer (pH 7.0) for three times by centrifugation at 15,000 rpm for 15 min. The DNA adsorption density was measured by the fluorescence signal of the DNA after dissolving the AuNPs with KCN (final 1 mM).[16] To test the colloidal stability of AuNPs, 5 M NaCl was add to 100 μL DNA-functionalized AuNPs to achieve a final NaCl concentration of 200, 400, and 600 mM. The color of the resulting AuNPs was documented using a digital camera.

Poly-A DNA stability assays. Poly-A DNA (1 μM) was incubated at different pH values for various amount of time. Then all the samples were adjusted to neutral pH before analyzed by 15% denaturing polyacrylamide gel electrophoresis (dPAGE). To test the possibility of forming apurinic (AP) sites, the A_{15} DNA (1 μM) was incubated under different pH's for 12 h. Then the samples were adjusted to neutral pH with 500 mM HEPES buffer, followed by adding a final of 1 μM T_{15} DNA for hybridization. After hybridization, SGI dye was added to stain the duplex DNA (ratio of DNA:SGI was 1:15). The same process was performed with the G_{15} DNA, except that C_{15} was added for hybridization. The final SGI fluorescence was measured by exciting at 485 nm and the emission was quantified at 535 nm.

Results and Discussion

Parallel poly-A DNA duplex at low pH. Before presenting our data, we first describe the salt-aging process to understand the surface chemistry of DNA adsorption (Figure 1A).[13, 17] Upon the initial mixing, only a few DNAs are adsorbed, both by the thiol group and the DNA bases. At a given ionic strength, an equilibrium is reached due to electrostatic repulsion between the adsorbed DNA and the DNA in solution. This equilibrium is shifted by raising the salt concentration to further screen the charge repulsion, allowing more DNA adsorption. Gradually, the DNA bases are displaced by the thiol groups of the newly adsorbed DNA (i.e. thiol affinity to gold is stronger than DNA base affinity), forcing each DNA to stand up. Finally, a highly stable conjugate is obtained, and the whole procedure usually requires a day or longer. In this salt-aging process, the spacer sequence (in green) does not play a critical role and it can be any nucleotide. Traditionally, a poly-A spacer was used.

At pH 3, the conjugation process can be completed in a few minutes.[19] In this case, a poly-A spacer is particularly useful.[26] With a pK_a of 3.5, adenine is partially protonated at pH 3 to decrease the negative charge density of DNA. While reduced charge repulsion is certainly helpful, the goal of this work is to examine the role of DNA conformation at low pH. For example, poly-A DNA can form the AH^+-H^+A base pair by a hydrogen bond between the N7 in one adenosine and the exocyclic amino group in another (Figure 1C).[33, 35] The consequence is the formation of a parallel poly-A duplex (i.e. A-motif).

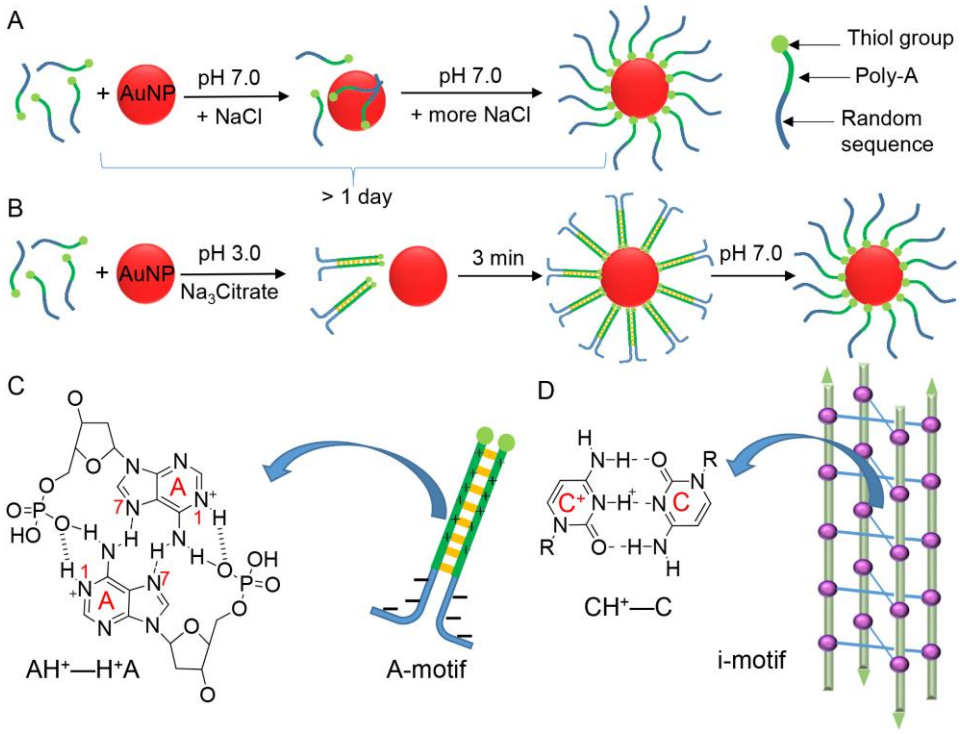

Figure 1. Schemes of adsorption of thiolated DNA onto AuNPs by (A) the salt-aging method and (B) the low-pH method. The formation of parallel poly-A duplex is highlighted in (B), leading to fully exposed thiol groups for AuNP attachment. (C) The base pairing scheme of AH^+-H^+A between two adenosines at low pH. The poly-A block can form a parallel duplex, and this duplex region is positively charged to favor its attachment to the gold surface. (D) The base pairing scheme of CH^+-C in the i-motif DNA.

With the parallel A-motif duplex in mind, two thiolated DNA can be held together by the green poly-A fragment in Figure 1B, exposing the thiol groups. This is only possible for a parallel DNA duplex so that the two thiol groups are on the same end. A further advantage is that the poly-A duplex region is positively charged, while the rest of the DNA is likely to be negatively charged (unless the rest of the DNA is purely poly-A/C). This favors selective adsorption of the thiolated

end due to electrostatic attraction with the negatively charged AuNP surface. Thus, such a rigid parallel duplex can also minimize internal DNA base adsorption, and the desired final structure can form just in one step (e.g. no need for thiol displacing DNA bases). All these factors may contribute to the fast DNA adsorption at low pH. The formation of A-motif can also explain the high loading density of non-thiolated poly-A DNA.[25, 26] In this paper, we describe our effort to confirm the role of such A-motif DNA during the conjugation reaction.

Characterizing the A-motif DNA by CD spectroscopy. Parallel poly-A duplexes have been studied in terms of biophysical properties,[36, 37] structure, [32, 33,38, 39] and analytical applications.[35, 40-42] Most previous work on used pure adenine homopolymers. In our system, however, the poly-A DNA is only a fraction of the whole sequence. In addition, there is also a fragment intended for DNA hybridization. To understand whether such DNA can form parallel duplex under our experimental conditions, circular dichroism (CD) spectroscopy was employed. The A_{15} DNA was first measured as a positive control. At pH 3.0, a characteristic positive CD peak at 268 nm was observed (Figure 2A), consistent with the previous literature report of parallel poly-A duplex.[32] When the pH is raised to 7.0, the peak at 223 nm increased strongly, while the peak at 268 nm disappeared, suggesting that the A-motif structure is disrupted. We next used a random DNA (DNA1 in Table 1) as a negative control. Its CD signal is quite weak and did not change much upon the pH drop (Figure 2B).

After these control experiments, we then tested three DNA sequences (DNA2-4); they all have the same random DNA sequence but with different lengths of the poly-A fragment. DNA with a longer poly-A fragment showed a more obvious decrease of the 223 nm peak upon the pH drop (Figure 2C-E). At the same time, the peak at 268 nm is stronger with longer poly-A, suggesting a longer poly-A block can better form the A-motif structure. The CD spectral difference

of DNA4 at these two pH's (Figure 2E) is not as large as that in the pure A_{15} DNA (Figure 2A), although they both contained an A_{15} fragment. This is likely due to the signal from the random sequence in DNA4 and DNA misfolding.

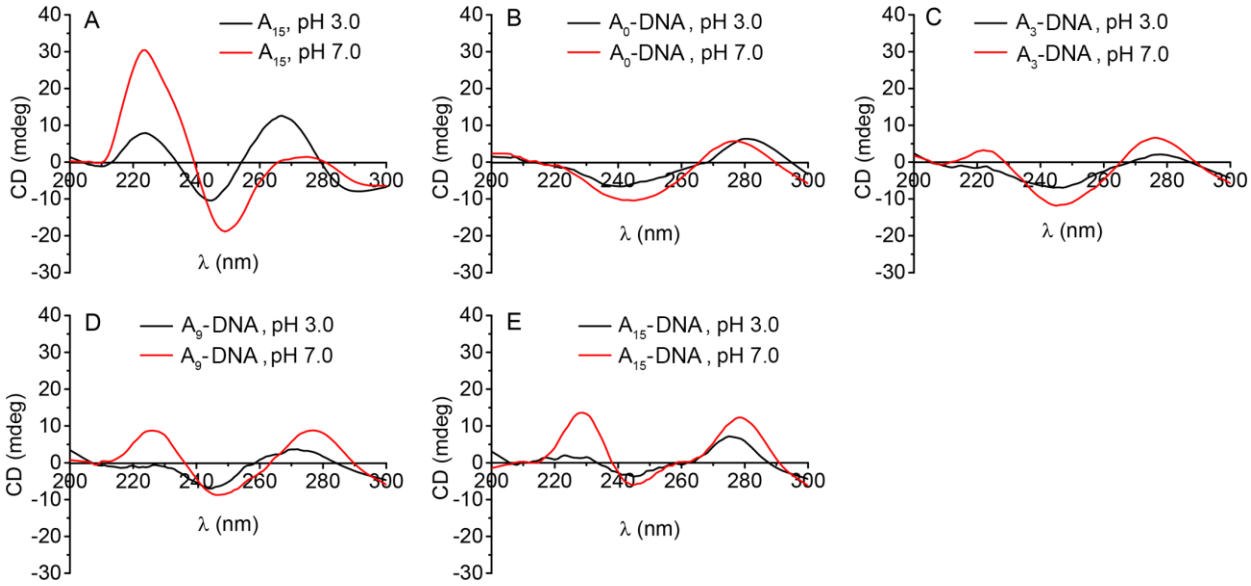

Figure 2. CD spectra of 10 μM DNA samples at pH 3.0 and 7.0 adjusted by 10 mM citrate buffer. (A) The A_{15} DNA (DNA9); (B) A_0-DNA (DNA1); (C) A_3-DNA (DNA2); (D) A_9-DNA (DNA3); and (E) A_{15}-DNA (DNA4).

Probing the A-motif by DNA staining dyes. Although CD spectroscopy is quite powerful, interpretation of its data is not often straightforward and this is not a very common instrument. Therefore, we also want to develop another method to study parallel poly-A in our system. For this purpose, a number of DNA staining dyes were screened, including SYBR Green I (SGI), ethidium bromide (EB), and thiazole orange (TO). SGI and EB did not produce a stronger fluorescence for a poly-A DNA at pH 3.0 than that at pH 7.0 (Figure S1, Supporting Information). Only TO (see Figure 3A for structure) showed a higher fluorescence with at pH 3.0 (Figure 3B).

At the same time, the fluorescence of TO stained poly-A DNA is quite stable at low pH for a day, while the fluorescence of this mixture only can maintain for ~1 h at pH 7.0 (Figure S2). This suggests that TO is protected by the poly-A structure at low pH from photobleaching. In contrast, TO is quite insensitive to pH for poly-T or poly-C DNA (Figure 3C, 3D). Poly-G DNA was not considered here, since they tend to form G-quadruplex and emit very strongly with TO.[43] TO is a useful dye for staining the A-motif if G-quadruplex can be excluded.

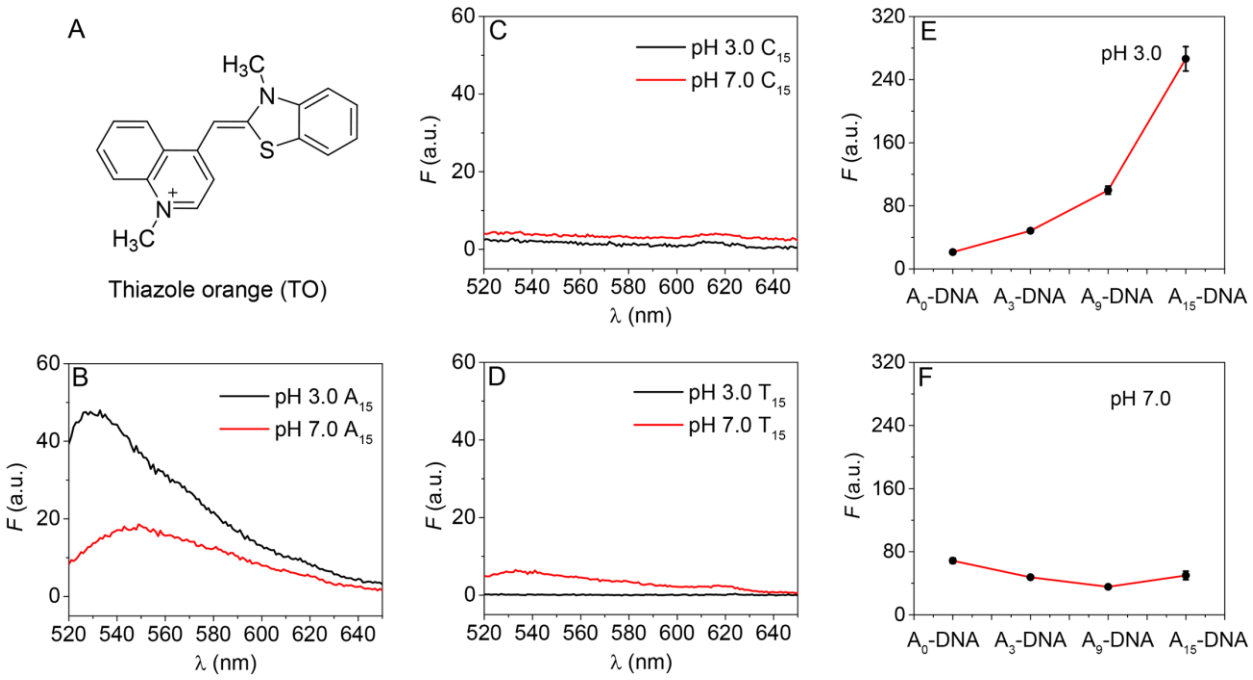

Figure 3. (A) The chemical structure of TO. Fluorescence spectra of TO stained (B) A_{15}, (C) C_{15}, and (D) T_{15} DNA at pH 3.0 and pH 7.0. The fluorescent intensity of TO stained DNA with different poly-A lengths (E) at pH 3.0 and (F) at pH 7.0. The ratio of DNA and TO molecule is 1:15 in all the samples.

We then tested the response of TO with DNA 1-4. The DNA with longer poly-A sequence has stronger fluorescent intensity (Figure 3E). This trend correlates well the length of poly-A suggesting the formation of parallel A-motif. At pH 7.0, fluorescent intensity is weak and independent of the length of poly-A (Figure 3F). Therefore, TO staining also supports that the A-motif can form in such DNA.

Order of mixing. The above CD and TO staining experiments indicate that poly-A DNA can form at pH 3.0, even with the appended 12-mer random DNA. This has strongly supported the model in Figure 1B. With this knowledge in mind, an interesting question is the order of mixing. So far, the protocol has been mixing the DNA and AuNPs first without adjusting pH, followed by adding pH 3.0 citrate buffer to a final of 10 mM. We call it post-acidification. We want to test the effect of acidifying DNA before mixing it with AuNPs (i.e. pre-acidification). This may give more time for A-motif formation.

We first tested two non-thiolated DNA. The A_{10} and A_{15} DNAs were chosen since this length range is often used as a spacer. In one group, DNA was mixed with AuNPs before adjusting the pH to 3.0 (Figure 4A). In another group, DNA was first incubated at pH 3.0 before adding AuNPs (Figure 4B). The stability of the resulting conjugates was measured by adding NaCl (Figure 4C, the first two groups). Individually dispersed AuNPs are red, while their color changes to blue/purple upon salt-induced aggregation. By simply observing the color, the colloidal stability of AuNPs can be judged. For both A_{10} and A_{15}, a better stability was achieved with the post-acidification method in Figure 4A. We further measured the loaded DNA density on AuNPs (Figure 4D). The DNA density trend is also consistent with the above stability measurement. It might be that during pre-acidification, a stable A-motif can form, resulting in most adenine nucleotides buried in the duplex and thus weaker interaction with the AuNP surface.[44] Since these

DNAs were non-thiolated and they require the adenine-AuNP interaction for adsorption, a lower stability was observed for the pre-acidification method.

To further understand it, we next used a few thiolated DNA each containing a A_9 spacer (DNA 16, 17). In this case, both methods yielded a similarly high stability (Figure 4C, the last two groups). With a thiol group, its interaction with the AuNP surface dominates the adenine base interaction. Overall, post-acidification appears to be the optimal method for non-thiolated DNA, while for thiolated DNA, either method should work.

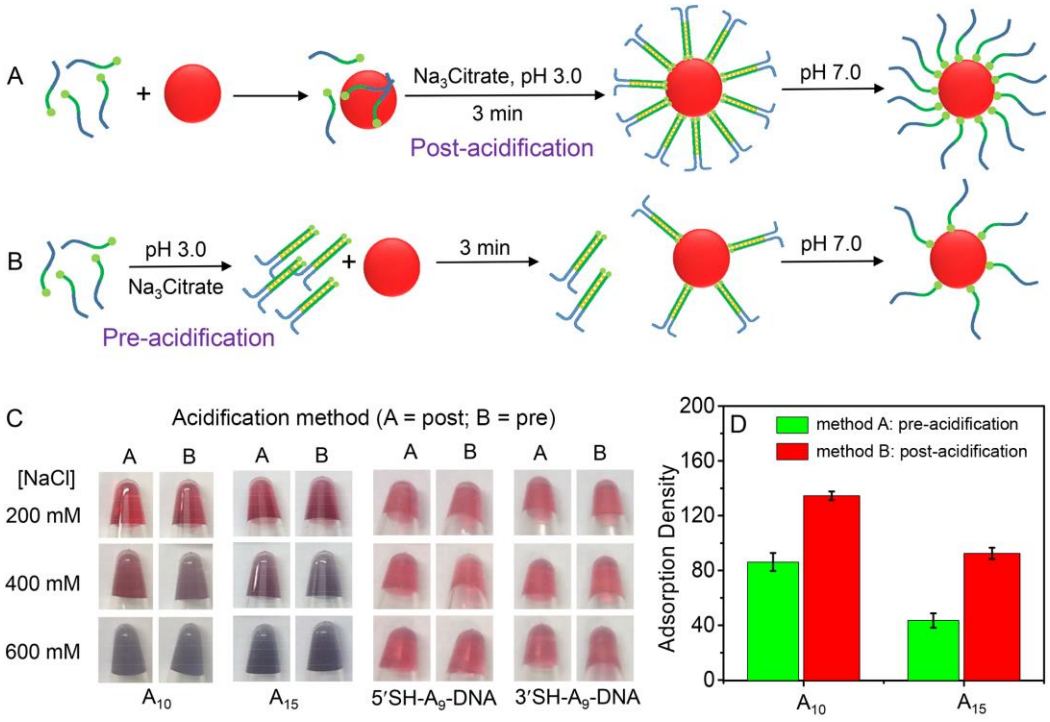

Figure 4. The schematic diagram of (A) mixing the DNA and AuNP before adjusting pH to 3 and (B) acidifying the DNA first to form the A-motif before adding AuNPs. The methods in (A) and (B) are called post- and pre-acidification, respectively. The final composition of these two samples are the same and only the order of mixing is different. The stability of the A_{10}, A_{15}, and two thiolated DNA with a A_9 spacer conjugated AuNPs assayed in different concentrations of NaCl

using the methods in (A) and (B), respectively. (D) The DNA adsorption density of A_{10} and A_{15} on AuNPs using these two methods.

DNA stability at low pH. At low pH, DNA may undergo depurination and then cleavage (Figure 5A).[45] Therefore, DNA is vulnerable at the adenine and guanine sites in acids. Since poly-A DNA is studied here, its stability at low pH is important to understand. To test this, we used FAM-labeled A_{15} and a random DNA (DNA15). These DNAs were incubated at various pH from 1.0 to 7.0 for 1 h and then analyzed using gel electrophoresis (Figure 5B and 5C). Neither the random DNA nor poly-A DNA was cleaved at pH 3.0 or even pH 1.0. Next, we incubated the FAM-A_{15} at pH 3.0 for up to 24 h, and still no degradation was observed (Figure 5D).

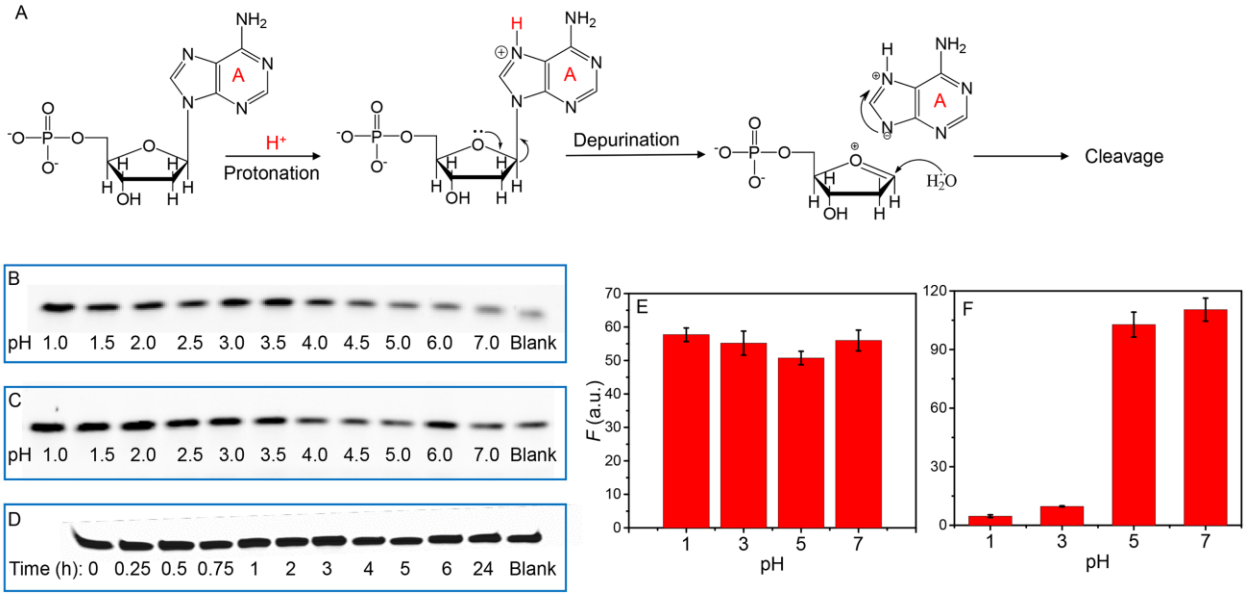

Figure 5. (A) The schematic diagram of the depurination reaction and subsequent DNA cleavage. At low pH, poly-purine DNAs such as poly-A and poly-G are unstable due to this reason. Gel electrophoresis micrographs showing the stability of (B) A_{15} and (C) a random DNA (DNA 15)

incubated at different pH values for 24 h, and (D) A_{15} incubated at pH 3.0 for various amount of time. The fluorescence intensity of (E) A_{15} and (F) G_{15} after incubation at various pH for 12 h and then hybridized with T_{15} or G_{15} at neutral pH to form duplex and finally stained with SGI.

The lack of cleavage products, however, may not fully exclude the possibility of apurinic sites (e.g. depurinated but not cleaved). To test this, we then designed a hybridization experiment. We incubated the A_{15} DNA in pH 1.0-7.0 buffers for 12 h. Then all the samples were brought to neutral pH and mixed with the same concentration of T_{15} to form duplex. Finally, SGI was added to stain the DNA, and all the samples showed a similar fluorescence intensity (Figure 5E). This result suggests that the A_{15} is still functional for hybridization and depurination is unlikely to happen. In contrast, the G_{15} DNA has lost its integrity at pH 3 or lower based on its hybridization with C_{15} and then staining (Figure 5F). The result is consistent with the longer half-life of A_{30} (97 h) than G_{18} (24 h) at pH 1.6. In the case of pH 2.5 at 37 °C, the half-life of A_{30} is 230 h.[46] For our conjugation method at pH 3, the stability of poly-A DNA is sufficient. However, we still need to be careful of the guanine nucleotides to keep them stable.

i-motif in poly-C DNA. In addition to adenine, cytosine (pK_a = 4.2) can also be protonated at pH 3. In addition, poly-C DNA may also form a unique structure called the 'i-motif' (Figure 1D). The i-motif has a characteristic CD spectrum with a dominant positive band at 290 nm and a negative band at around 260 nm.[47] Using a series of poly-C containing DNA (DNA 5-8), we measured their CD spectra using the same condition as the poly-A DNA. First, the random DNA was measured to understand the background signal (Figure 6A). Then, the length of poly-C block was increased in the DNA (Figure 6B-D), where the positive peak at 290 nm and the negative peak at 260 became stronger at pH 3. This change supports the formation of i-motif structure even when the poly-C

DNA is appended with a block of random sequence. The i-motif is a less favorable secondary structure for the DNA conjugation reaction since it contains four DNA strands arranged in an overall anti-parallel manner (Figure 1D). This may explain the difficulties associated with forming functional conjugates we previously reported for non-thiolated poly-C containing DNA.[26]

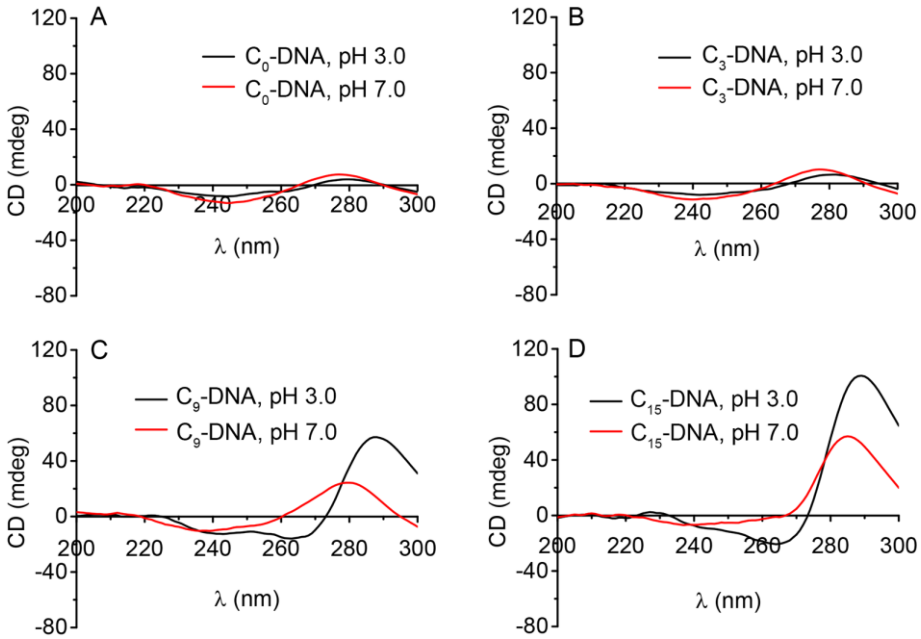

Figure 6. CD spectra of 10 μM DNA samples at pH 3.0 and 7.0 in 10 mM citrate buffer. (A) C_0-DNA (DNA5); (B) C_3-DNA (DNA6); (C) C_9-DNA (DNA7); and (D) C_{15}-DNA (DNA8).

Further discussion. In this study, we confirmed the role of the parallel poly-A duplex at low pH in assisting the conjugation reaction. This method works for both thiolated and non-thiolated DNA, as long as they contain a block of poly-A DNA. For thiolated DNA, a high DNA density can be easily rationalized. At low pH, both thermodynamic and kinetic effects are favorable for achieving a high density of DNA with the intended DNA conformation. There is no need for the thiol group

to displace adsorbed DNA bases. This is why this low pH method works so well for thiolated DNA with a poly-A block. For non-thiolated DNA, the kinetic factor dominates initially. Although adenine can displace other bases especially thymine, it is not as efficient as thiol displacing DNA bases.[15] Forming the A-motif at low pH can also help non-thiolated DNA to be adsorbed in the intended conformation.

This study has also implication on DNA sequence design for the bioconjugation reaction. In retrospect, it was quite lucky that we followed Mirkin's sequence design to involve a block of poly-A sequence as spacer in our experiment.[19] After observing the interesting effect of low pH, we initially attributed it to a simple electrostatic model. In this work, we emphasized also on the effect of DNA conformation, which allowed us to explain the difference between poly-A and poly-C spacer,[26] and also the adsorption of non-thiolated DNA. Now that the importance of the parallel poly-A is confirmed, we can intentionally design sequences to contain poly-A instead of poly-C. Using a poly-T spacer might work well with the salt-aging method but it is unlikely to be a good choice for the low-pH method since thymine cannot be protonated. Poly-G may also fold to complex quadruplex structures and cannot be protonated either unless pH is lower than 2, where guanine nucleotide is expected to suffer from depurination and cleavage. In addition to poly-A, some other special sequences may also form parallel duplexes. This however require two different strands of carefully designed sequences.[48] Their contribution to DNA adsorption to AuNPs is less easy to generalize.

Conclusions

In summary, the roles of parallel poly-A duplex in DNA adsorption at low pH were studied in this work. The formation of such A-motifs in DNA sequences containing only a block of adenine (and the rest are random sequences) is supported by CD spectroscopy. We further screened a few DNA staining dyes showing that TO can selectively detect the A-motif at low pH. While the previous understanding was focused on electrostatic interactions, this work shows the unique role of DNA conformation. The order of mixing DNA and AuNPs and pH adjustment has also been optimized. For non-thiolated DNA, the optimal attachment is achieved by mixing poly-A DNA and AuNPs at neutral pH followed by pH adjustment. For thiolated DNA, adjusting pH either before or after mixing DNA with AuNPs can work. For the same conformational reasons, poly-C DNAs forming i-motif are less favorable for the low pH method. Finally, we confirmed that poly-A DNA is very stable under the acidic pH conditions for the AuNP conjugation reaction, while the stability of poly-G DNA is lower due to the depurination reaction. This work has provided new insights into the reaction between DNA and AuNPs, and it will facilitate related research in biosensor development and nanotechnology. While the current discussion is made with AuNPs, the formation of A-motif at low pH is independent of gold. Bearing this in mind, it is also possible to design poly-A DNA sequences at low pH for interacting with other surfaces.

Acknowledgement

Funding for this work is from The Natural Sciences and Engineering Research Council of Canada (NSERC).

References

1. Rosi, N. L.; Mirkin, C. A., Nanostructures in Biodiagnostics. *Chem. Rev.* **2005,** 105, 1547-1562.
2. Liu, J.; Cao, Z.; Lu, Y., Functional Nucleic Acid Sensors. *Chem. Rev.* **2009,** 109, 1948-1998.
3. Zhao, W.; Brook, M. A.; Li, Y., Design of Gold Nanoparticle-Based Colorimetric Biosensing Assays. *ChemBioChem* **2008,** 9, 2363-2371.
4. Song, S.; Qin, Y.; He, Y.; Huang, Q.; Fan, C.; Chen, H.-Y., Functional Nanoprobes for Ultrasensitive Detection of Biomolecules. *Chem. Soc. Rev.* **2010,** 39, 4234-4243.
5. Wilner, O. I.; Willner, I., Functionalized DNA Nanostructures. *Chem. Rev.* **2012,** 112, 2528-2556.
6. Wang, H.; Yang, R.; Yang, L.; Tan, W., Nucleic Acid Conjugated Nanomaterials for Enhanced Molecular Recognition. *ACS Nano* **2009,** 3, 2451-2460.
7. Giljohann, D. A.; Seferos, D. S.; Daniel, W. L.; Massich, M. D.; Patel, P. C.; Mirkin, C. A., Gold Nanoparticles for Biology and Medicine. *Angew. Chem., Int. Ed.* **2010,** 49, 3280-3294.
8. Torabi, S.-F.; Lu, Y., Functional DNA Nanomaterials for Sensing and Imaging in Living Cells. *Curr. Opin. Biotechnol.* **2014,** 28, 88-95.
9. Pinheiro, A. V.; Han, D.; Shih, W. M.; Yan, H., Challenges and Opportunities for Structural DNA Nanotechnology. *Nat. Nanotechnol.* **2011,** 6, 763-772.
10. Liu, W.; Tagawa, M.; Xin, H. L.; Wang, T.; Emamy, H.; Li, H.; Yager, K. G.; Starr, F. W.; Tkachenko, A. V.; Gang, O., Diamond Family of Nanoparticle Superlattices. *Science* **2016,** 351, 582-586.

11. Jones, M. R.; Seeman, N. C.; Mirkin, C. A., Programmable Materials and the Nature of the DNA Bond. *Science* **2015,** 347, 1260901.

12. Tan, L. H.; Xing, H.; Lu, Y., DNA as a Powerful Tool for Morphology Control, Spatial Positioning, and Dynamic Assembly of Nanoparticles. *Acc. Chem. Res.* **2014,** 47, 1881-1890.

13. Herne, T. M.; Tarlov, M. J., Characterization of DNA Probes Immobilized on Gold Surfaces. *J. Am. Chem. Soc.* **1997,** 119, 8916-8920.

14. Storhoff, J. J.; Elghanian, R.; Mirkin, C. A.; Letsinger, R. L., Sequence-Dependent Stability of DNA-Modified Gold Nanoparticles. *Langmuir* **2002,** 18, 6666-6670.

15. Kimura-Suda, H.; Petrovykh, D. Y.; Tarlov, M. J.; Whitman, L. J., Base-Dependent Competitive Adsorption of Single-Stranded DNA on Gold. *J. Am. Chem. Soc.* **2003,** 125, 9014-9015.

16. Demers, L. M.; Mirkin, C. A.; Mucic, R. C.; Reynolds, R. A.; Letsinger, R. L.; Elghanian, R.; Viswanadham, G., A Fluorescence-Based Method for Determining the Surface Coverage and Hybridization Efficiency of Thiol-Capped Oligonucleotides Bound to Gold Thin Films and Nanoparticles. *Anal. Chem.* **2000,** 72, 5535-5541.

17. Cutler, J. I.; Auyeung, E.; Mirkin, C. A., Spherical Nucleic Acids. *J. Am. Chem. Soc.* **2012,** 134, 1376-1391.

18. Zhang, X.; Servos, M. R.; Liu, J., Surface Science of DNA Adsorption onto Citrate-Capped Gold Nanoparticles. *Langmuir* **2012,** 28, 3896-3902.

19. Zhang, X.; Servos, M. R.; Liu, J., Instantaneous and Quantitative Functionalization of Gold Nanoparticles with Thiolated DNA Using a pH-Assisted and Surfactant-Free Route. *J. Am. Chem. Soc.* **2012,** 134, 7266-7269.

20. Zhang, X.; Gouriye, T.; Göeken, K.; Servos, M. R.; Gill, R.; Liu, J., Toward Fast and Quantitative Modification of Large Gold Nanoparticles by Thiolated DNA: Scaling of Nanoscale Forces, Kinetics, and the Need for Thiol Reduction. *J. Phys. Chem. C* **2013,** 117, 15677-15684.

21. Ohta, S.; Glancy, D.; Chan, W. C. W., DNA-Controlled Dynamic Colloidal Nanoparticle Systems for Mediating Cellular Interaction. *Science* **2016,** 351, 841-845.

22. Shi, D.; Song, C.; Jiang, Q.; Wang, Z.-G.; Ding, B., A Facile and Efficient Method to Modify Gold Nanorods with Thiolated DNA at a Low pH Value. *Chem. Commun.* **2013,** 49, 2533-2535.

23. Zhang, X.; Servos, M. R.; Liu, J., Fast pH-Assisted Functionalization of Silver Nanoparticles with Monothiolated DNA. *Chem. Commun.* **2012,** 48, 10114-6.

24. Zhou, W.; Ding, J.; Liu, J., A Platinum Shell for Ultraslow Ligand Exchange: Unmodified DNA Adsorbing More Stably on Platinum Than Thiol and Dithiol on Gold. *Chem. Commun.* **2015,** 51, 12084-7.

25. Zhang, X.; Liu, B.; Dave, N.; Servos, M. R.; Liu, J., Instantaneous Attachment of an Ultrahigh Density of Nonthiolated DNA to Gold Nanoparticles and Its Applications. *Langmuir* **2012,** 28, 17053-17060.

26. Zhang, X.; Liu, B.; Servos, M. R.; Liu, J., Polarity Control for Nonthiolated DNA Adsorption onto Gold Nanoparticles. *Langmuir* **2013,** 29, 6091-6098.

27. Opdahl, A.; Petrovykh, D. Y.; Kimura-Suda, H.; Tarlov, M. J.; Whitman, L. J., Independent Control of Grafting Density and Conformation of Single-Stranded DNA Brushes. *Proc. Natl. Acad. Sci. U. S. A.* **2007,** 104, 9-14.

28. Pei, H.; Li, F.; Wan, Y.; Wei, M.; Liu, H.; Su, Y.; Chen, N.; Huang, Q.; Fan, C., Designed Diblock Oligonucleotide for the Synthesis of Spatially Isolated and Highly Hybridizable Functionalization of DNA–Gold Nanoparticle Nanoconjugates. *J. Am. Chem. Soc.* **2012,** 134, 11876-11879.

29. Tan, L. H.; Yue, Y.; Satyavolu, N. S. R.; Ali, A. S.; Wang, Z.; Wu, Y.; Lu, Y., Mechanistic Insight into DNA-Guided Control of Nanoparticle Morphologies. *J. Am. Chem. Soc.* **2015,** 137, 14456-14464.

30. Shen, J.; Xu, L.; Wang, C.; Pei, H.; Tai, R.; Song, S.; Huang, Q.; Fan, C.; Chen, G., Dynamic and Quantitative Control of the DNA-Mediated Growth of Gold Plasmonic Nanostructures. *Angew. Chem., Int. Ed.* **2014,** 53, 8338-8342.

31. Song, T.; Tang, L.; Tan, L. H.; Wang, X.; Satyavolu, N. S. R.; Xing, H.; Wang, Z.; Li, J.; Liang, H.; Lu, Y., DNA-Encoded Tuning of Geometric and Plasmonic Properties of Nanoparticles Growing from Gold Nanorod Seeds. *Angew. Chem., Int. Ed.* **2015,** 54, 8114-8118.

32. Chakraborty, S.; Sharma, S.; Maiti, P. K.; Krishnan, Y., The Poly dA Helix: A New Structural Motif for High Performance DNA-Based Molecular Switches. *Nucleic Acids Res.* **2009,** 37, 2810-2817.

33. Safaee, N.; Noronha, A. M.; Rodionov, D.; Kozlov, G.; Wilds, C. J.; Sheldrick, G. M.; Gehring, K., Structure of the Parallel Duplex of Poly(A) RNA: Evaluation of a 50 Year-Old Prediction. *Angew. Chem., Int. Ed.* **2013,** 52, 10370-10373.

34. Liu, J.; Lu, Y., Preparation of Aptamer-Linked Gold Nanoparticle Purple Aggregates for Colorimetric Sensing of Analytes. *Nat. Protoc.* **2006,** 1, 246-252.

35. Saha, S.; Chakraborty, K.; Krishnan, Y., Tunable, Colorimetric DNA-Based pH Sensors Mediated by A-Motif Formation. *Chem. Commun.* **2012,** 48, 2513-5.

36. Jissy, A.; Konar, S.; Datta, A., Molecular Switching Behavior in Isosteric DNA Base Pairs. *ChemPhysChem* **2013,** 14, 1219-1226.

37. Holm, A. I. S.; Munksgaard Nielsen, L.; Vrønning Hoffmann, S.; Brøndsted Nielsen, S., On the Formation of the Double Helix between Adenine Single Strands at Acidic pH from Synchrotron Radiation Circular Dichroism Experiments. *Biopolymers* **2012,** 97, 550-557.

38. Choi, J.; Majima, T., Conformational Changes of Non-B DNA. *Chem. Soc. Rev.* **2011,** 40, 5893-5909.

39. Kim, S.; Choi, J.; Majima, T., Self-Assembly of Polydeoxyadenylic Acid Studied at the Single-Molecule Level. *J. Phys. Chem. B* **2011,** 115, 15399-405.

40. Zheng, B.; Cheng, S.; Liu, W.; Lam, M. H.; Liang, H., A Simple Colorimetric pH Alarm Constructed from DNA-Gold Nanoparticles. *Anal. Chim. Acta* **2012,** 741, 106-113.

41. Wang, C.; Tao, Y.; Pu, F.; Ren, J.; Qu, X., pH-Responsive DNA Assembly Regulated through A-Motif. *Soft Matter* **2011,** 7, 10574-10580.

42. Saha, S.; Bhatia, D.; Krishnan, Y., pH-Toggled DNA Architectures: Reversible Assembly of Three-Way Junctions into Extended 1D Architectures through A-Motif Formation. *Small* **2010,** 6, 1288-1292.

43. Lubitz, I.; Zikich, D.; Kotlyar, A., Specific High-Affinity Binding of Thiazole Orange to Triplex and G-Quadruplex DNA. *Biochemistry* **2010,** 49, 3567-3574.

44. Bano, F.; Sluysmans, D.; Wislez, A.; Duwez, A.-S., Unraveling the Complexity of the Interactions of DNA Nucleotides with Gold by Single Molecule Force Spectroscopy. *Nanoscale* **2015,** 7, 19528-19533.

45. Suzuki, T.; Ohsumi, S.; Makino, K., Mechanistic Studies on Depurination and Apurinic Site Chain Breakage in Oligodeoxyribonucleotides. *Nucleic Acids Res.* **1994,** 22, 4997-5003.

46. An, R.; Jia, Y.; Wan, B.; Zhang, Y.; Dong, P.; Li, J.; Liang, X., Non-Enzymatic Depurination of Nucleic Acids: Factors and Mechanisms. *PLoS One* **2014,** 9, e115950.

47. Kypr, J.; Kejnovská, I.; Renčiuk, D.; Vorlíčková, M., Circular Dichroism and Conformational Polymorphism of DNA. *Nucleic Acids Res.* **2009,** 37, 1713-1725.

48. Parvathy, V. R.; Bhaumik, S. R.; Chary, K. V. R.; Govil, G.; Liu, K.; Howard, F. B.; Miles, H. T., Nmr Structure of a Parallel-Stranded DNA Duplex at Atomic Resolution. *Nucleic Acids Res.* **2002,** 30, 1500-1511.